Histological Study for the Possible Protective Role of Zinc Oxide Nanoparticles and Vitamin E on Testis from Cisplatin-Induced Injury in Adult Albino Rats

Abstract

Background: Cisplatin (CP) is a standard chemotherapy that is commonly applied in the cure of testicular cancer. Zinc oxide nanoparticles (ZnO-NPs) are metal oxides known for their antioxidant activities. Vitamin E has been known for its protective effects against oxidative stress-induced damage. **The study's aim:** This research focused on assessing the potential protective effect of ZnO-NPs and vitamin E against testicular damage caused by CP**. Materials and Methods:** This experimental study was conducted in the Anatomy Department at Benha University between January 2024 and February 2024. Fifty adult male rats divided into 5 equivalent groups: group I (controls), group II (CP), group III (CP + ZnO-NPs), group IV (CP + vitamin E), and group V (CP + ZnO-NPs + vitamin E). Testes specimens were taken and prepared for examination by light and electron microscope. **Results:** light and electron microscopic examination showed distorted architecture with degeneration & necrosis in group II. Group III showed limited distortion, degeneration and necrosis. Group IV showed some damage. Group V appeared nearly normal. Morphometric study showed a notable decline ($P< 0.01$) in mean area % of groups III, IV, and V in comparison to group II. Group V had the most significant reduction. **Conclusion**: ZnO-NPs and vitamin E, whether used separately or together, can significantly safeguard the testes from damage caused by CP by reducing oxidative stress. ZnO-NPs demonstrate superior results compared to vitamin E; however, the co-administration of both ZnO-NPs and vitamin E shows a greater improvement in efficacy than ZnO-NPs used alone.

Keywords: Histological; Protective Role; Zinc Oxide Nanoparticles; Vitamin E, Cisplatin-Induced Injury.

Introduction

Tools and techniques based on nanomaterials are advancing quickly in biomedicine[1]. Zinc oxide nanoparticles (ZnO-NPs), approved by the FDA as safe, are notable among these materials [2, 3]. Zinc itself is essential for testicular development, function, and spermatogenesis [4, 5].

Cisplatin (CP) is one of the major standard anticancer drugs that is widely used in treatment of solid tumors such as tumor of the testis. However, it has severe reproductive toxicity especially in males [6, 7].

CP inhibits cell division and induces apoptosis by joining DNA. Also, it increases the reactive oxygen species (ROS), leading to increased oxidative insult. This condition is

marked by up-regulated lipid peroxidation and down-regulated levels of antioxidant defensive enzymes [8].

Combining antioxidants with chemotherapy (CP) can reduce its toxicity and improve treatment outcomes [4].

Vitamin E is an essential element of the non-enzymatic antioxidant defense system. It has many functions, including: supporting enzymatic activity, regulating genes, and inhibiting platelet aggregation [9]. Vitamin E acts as a free radical scavenger, alleviating cell membranes and maintaining their permeability [10].

The purpose of our research was to explore the probable defensive role of ZnO-NPs and Vit-E on testes from CP induced injury of adult albino rats.

Drugs and methods

Drugs and chemicals:

CP was acquired from **Pfizer Chemical Company (USA)** in vial form and is produced by **Mylan in France**. **CAS. Number:** 15663-27-1. The infusion concentrate in each vial is 50 ml with (1 mg/mL CP), 9 mg/mL NaCl, HCL, and NaOH to bring the pH down to about 4.0, and H2O for injection to reach a total volume of 50 ml. Rats were housed for 4 weeks after receiving a single dose of the medication intraperitoneally (IP) at dose of 8 mg/kg [11].

The supplier of ZnO-NPs was **Nano Gate Company,** located at **9254 Huda Shaarawy St., Mokattam, Cairo, Egypt. CAS. Number:** 1314-13-2. The powder was white to yellow in color, was 30 ±5 nm in size, had a molecular wt of 81.408 gm/mol, and had a purity of over 99.9%. For five weeks, each rat received injected IP/day of ZnO-NPs (5 mg/kg/day) beginning one week before the CP dose and continuing for four weeks following the CP [4].

Vit E (400 mg) was brought in the form of capsules of yellow oily material from **Pharco Company, Amriya, Alexandria, Egypt. CAS. Number:** 10191-41-0. It was given in (100 mg/ kg/ every day) orally by gastric intubation for 5 weeks starting 1week prior the dose of CP & then continued it for 4 weeks after CP [12].

Animals of the study:

This histological study involved 50 healthy adult male albino rats aged about eight-ten weeks and weighing (185-220 g). The rats were brought from the animal house-Moshtohor Faculty of Veterinary Medicine, Benha University and utilized according to the lab strategies of animal's care under approval number: **(MS 15-2-2023)** from the Institutional Animal Care Committee.

Experimental Design:

An experimental animal study was done from January 2024 to February 2024.The dose was adjusted according to the individual rat's weight. After five weeks of housing, the rats (50) were divided into 5 groups, 10 rats/group (n=10):

Group I (control group): 10 rats evenly divided into five sub-groups:

Ia: 2 rats that given no treatments.

Ib (serving as a control group for CP injection): 2 rats received an intraperitoneal (IP) injection of 0.9% NaCl at a rate of (8 ml/ kg/ day) administered once during the experiment.

Ic (serving as a control group for CP and ZnO-NPs injection): 2 rats received an IP injection of normal saline, similar to group Ib, and were also given IP normal saline at a dosage of (5 ml /k g/daily) for a duration of five weeks.

Id (serving as a control group for CP and vit E): Two rats were administered IP with normal saline similar to group Ib and received a sunflower oil solution orally via a gastric tube at a dosage of (100 mg/kg/daily) for five weeks.

Ie (serving as a control group for CP+ ZnO-NPs+ vit E): 2 rats received IP injections of normal saline as in group Ic and a sunflower oil solution as in group Id.

Group II (CP group): rats received one IP injection of CP (8 mg/kg) and were observed for 4 weeks.

Group III (CP + ZnO-NPs group): rats received one IP injection of CP as in group II and were given ZnO-NPs (5 mg/kg/day), beginning ZnO-NPs one week prior to the CP dose and continuing for 4 weeks after CP [4].

Group IV (CP + vitamin E group): rats received one IP injection of a single dose of CP as in group II and were administered oral vitamin E (100 mg/kg/day), beginning one week prior to the CP dose and continuing for 4 weeks after CP [12].

Group V (CP + ZnO-NPs + vitamin E group): rats received one IP injection of CP as in group II and ZnO-NPs as IP injection along with oral vitamin E at the similar doses as in groups III and IV, beginning one week prior to the CP dose and maintaining the treatments for 4 weeks post-CP.

Sampling:

Rats were anesthetized by ether and cervical decapitated after four weeks from CP injection in groups II, III, IV and V & 5 weeks in group I, then testis specimens were obtained from rats of experimental groups, then the animals were eliminated by incineration in Benha University Hospital incinerator.

Histological methods:

Hematoxylin and Eosin staining for histological evaluation: testicular samples were dipped in 10% formalin and handled for preparing paraffin sections of (5-7 µm thick), fixed on glass slides for H&E. Sections prepared according to standard protocol [13]. Results: the nuclei were blue and the cytoplasm was pink.

Masson's Trichrome for collagen fibrotic changes: Other sections were treated with Masson's Trichrome as Bancroft and Lyton as a reference [13]. Results: the nuclei were blue-black, the cytoplasm, muscle and RBCs were red and the collagen was blue.

Transmission electron microscope technique (TEM):

Small tissue sections were cut into slices and fixed immediately in buffered formol-glutaraldehyde for 24 hs to preserve the ultrastructure. Semi-thin sections were treated with Toluidine blue. Later, ultrathin sections (80 nm thick) were obtained from certain areas using glass knife. All steps were carried according to standard protocol [14]. Grids were scanned and images were captured by TEM (Joel/JEM/100 SX electron microscope) in EM Unit, Faculty of Medicine at Tanta University.

Morphometric study:

The average of collagen fiber area % deposition (Masson trichrome stain) was measured in ten images from ten distinct fields for each group of rats utilizing Image-Pro Plus software version 6 (Media Cybernetics Inc., Bethesda, Maryland, USA). The digital photos were obtained by Leica DM-500 optical microscopes- Histology department, Benha faculty of Medicine.

Approval code: (MS 15-2-2023)

Statistical analysis:

The obtained data were analyzed carefully using windows statistical software IBM SPSS, Version 23 (IBM Corp., USA). Morphometric results were compared for variations with a one-way analysis of variance (ANOVA) then Post Hoc LSD test; in every test, the data were explained as the mean (M) value, standard deviation (SD), and changes were supposed significant at $P < 0.01$.

Results

Histological studies:

By light microscope:

H&E results (Figure 1-I):

The usual architecture of seminiferous tubules divided by interstitial tissue (including clusters of Leydig cells) was observed in group I (control group), (**Figs: IA- IB).**

In group II, the distorted architecture of seminiferous tubules was revealed, along with degeneration, vacuolation, shedding of germinal epithelium, necrotic germ cells in the tubule's center, and decreased sperms appearance. The interstitial tissue also displayed vacuoles and congestion, and the blood vessels between the seminiferous tubules appeared dilated and clogged, **(Figs: IC-ID).**

Significantly better seminiferous tubules with regular outlines were seen in group III. With some vacuolations, the tubules were narrow-spaced and lined with integral stratified germinal epithelium, and minor vacuolations. There are still some exudate fluid and vacuoles in the interstitial tissue, **(Figs: IE-IF).**

Group IV showed reduced but still notable seminiferous tubule damage, with disturbed outlines and partial germ cell loss. Tubules exhibited vacuolation, cell shedding, and basement membrane discontinuity. Interstitial tissue showed vacuoles, exudate, vascular congestion, and inflammatory cells, **(Figs: IG-IH).**

In group V, the seminiferous tubules were almost identical to normal. A thick layer of intact stratified germinal epithelium coated the tubules, which seemed to be adhering to the BM. The seminiferous tubules' spermatogenic cells displayed every stage of spermatogenesis, from outward to inward, with mature spermatozoa filling the lumen (spermatogonia, primary spermatocytes, spermatids). There were clusters of normal Leydig cells with few vacuoles and exudation in the interstitial spaces, **(Figs: I I-IJ).**

Masson trichrome results (Figure 1-II):

In group I**:** The Masson's trichrome stained tissues of this group showed the regular spreading of fine collagen fibres at the BM of seminiferous tubules, perivascular and in between the tubules, **(Fig: II-A).** Group II: revealed marked accumulation of dense collagen fibers at the BM of seminiferous tubules, in the wall of the vasculature and in between the tubules, **(Fig: II-B).** Group III: showed collagen fibers accumulation at the BM of seminiferous tubules and in-between the seminiferous tubules, **(Fig: II-C).** Group IV: accumulation of collagen fibers at the BM of seminiferous tubules, around the enlarged vasculature and in the interstitial tissue in-between the seminiferous tubules, **(Fig: II-D).** Group V: deposition of fine collagen fibers at the BM of seminiferous tubules, perivascular and in between the tubules, **(Fig: II-E).**

Morphometric results:

In comparison to group II, the mean area % of groups III, IV, and V decreased significantly ($P<0.01$). In comparison to each of groups III and IV, the mean area percentage of groups V decreased significantly ($P<0.01$), but it was still lesser than that of group I (**Table 1).**

Table 1: Table Shows the mean area percentage and SD of collagen fiber accumulation in each group, compared across all groups using the Post Hoc LSD test

	Group I	Group II	Group III	Group IV	Group V
Mean area %	1.72%	7.25%	3.42%	5.57%	2.42%
SD	0.2725	0.5087	0.4684	0.3931	0.2231
Significance at P < 0.01	2,3,4,5	1,3,4,5	1,2,4,5	1,2,3,5	1,2,3,4

Data represented as star (SD) or frequency, e with group I, 2=significance with group II, 3=signifi p III, 4=significan V, 5=significance with group V

TEM results:

Group I: Electron microscopic examination revealed seminiferous tubules surrounded by one layer of myoid cells with normal structure of cells, Sertoli cells in **Fig. (2A),** Spermatogonia in **Fig. (2B),** 1ry spermatocytes in **Fig. (2C)** and spermatids with acrosomal vesicle and Cap in **Fig. (2D).** longitudinal section of sperms showed the pyriform shaped nucleus covered anteriorly by acrosomal cap and posteriorly by caudal sheath of the tail and cut section of sperm had: 1) principal piece 2) middle piece and 3) end piece in **Fig. (2E),** and interstitial tissue showed Leydig cell in **Fig. (2F).**

Group II: showed widespread degeneration of seminiferous epithelium. Sertoli and germ cells had nuclear damage, cytoplasmic vacuolation, and swollen organelles. Sperm and Leydig cells were severely deformed with structural and mitochondrial damage. **Fig. (3A):** showed Sertoli cell changes. **Fig. (3B):** changes in Spermatogonia. **Fig. (3C):** Primary spermatocytes with nuclear and mitochondrial changes. **Fig. 3D:** distorted Spermatids with nuclear and cytoplasmic changes. **Fig. (3E):** Longitudinal section of sperms showed distortion and disassembly. **Fig. (3F):** Leydig cells changes.

Group III: Showed better tubular structure with slightly thickened basement membranes. Sertoli and germ cells appeared near normal, with some vacuolations and swollen mitochondria. Spermatids and sperm showed minimal abnormalities, and Leydig cells had moderate mitochondrial and nuclear changes. **Figs. (4A-4B):** Sertoli cells and spermatogonia cells. **Fig. (4C):** Primary spermatocytes showed a very important sign of improvement: autophagosome. **Fig. (4D):** Spermatid showed with some changes. **Fig. (4E):** longitudinal section of sperm. **Fig. (4F):** Leydig cell with nuclear and cytoplasmic changes.

Group IV: revealed persistent degeneration in Sertoli, spermatogonia, and spermatocyte cells. Spermatids and sperm showed structural deformities, and Leydig cells displayed swollen mitochondria and nuclear abnormalities. Generally better than Group II but less than Group III. **Fig. (5A):** showed Sertoli cell. **Fig. (5B):** spermatogonia cell. **Fig. (5C):**

Primary spermatocyte. **Fig. (5D):** Spermatid. **Fig. (5E):** longitudinal sections of sperms. **Figure 5F:** Leydig cell with ill-defined cell boundary.

Group V: Showed semi-normal seminiferous tubule structure with normal Sertoli, spermatogonia, and spermatocyte cells. Spermatids and sperm appeared normal, and Leydig cells showed healthy organelles and lipid droplets. **Fig. (6A):** Sertoli cell resting over thin BM. **Fig. (6B):** Spermatogonia were seen lying on basement membrane. **Fig. (6C):** Primary spermatocytes. **Fig. (6D):** Normal spermatid with acrosomal cap on part of nucleus. **Fig. 6E:** Longitudinal section of sperms showed the pyriform shaped nucleus covered anteriorly by acrosomal cap and posteriorly by caudal sheath of the tail. **Fig. (6F):** Leydig cell appeared nearly normal with multiple mitochondria and many lipid droplets of variable sizes.

Discussion

It has been proved that testicular function is reduced due to oxidative insult, inflammation, and germ cell loss, which are the causes behind CP-induced testicular damage. When antioxidant defenses and reactive oxygen radicles production are out of equilibrium, oxidative stress results. Increased ROS levels brought on by CP therapy have been demonstrated to cause lipid peroxidation and cellular structural damage [15]. Because ZnO-NPs and vitamin E have comparable modes of action, they may work in concert to protect testicular tissue from oxidative damage [16].

In line with our results concerning disruption and degeneration of testicular cells and increased collagen in Group II (CP- Treated), Ismail et al. [17] indicated that CP exposure leads to an imbalance in antioxidant defenses, resulting in up-regulated malondialdehyde (MDA) and down-regulated glutathione (GSH) in testicular sections. This oxidative stress was linked to degeneration of germ cells and alterations in sperm parameters. Also, Abdel-Latif et al. [15] stated that CP treatment resulted in azoospermia (absence of sperm) and significant histological changes in testicular architecture, including deteriorated tubules and increased collagen deposition. These changes were attributed to CP- induced inflammation as well as oxidative stress.

The observed vacuolation and fluid exudate in interstitial tissue suggest an inflammatory response to cellular injury. Also, damage to the germinal epithelium disrupts the normal process of sperm production, leading to decreased sperm count and necrosis of germ cells [18, 19]. Moreover, the enlarged spaces in-between germ cells and loss of interaction between them, according to Gong et al. [20], are likely caused by disruptions of Sertoli cells that in turn result in the loss of germ cells, testicular tissue damage, and infertility.

On the other hand, lipid peroxidation is the primary cause of intracellular H2O accumulation, which leads to the creation of vacuoles and the dilatation of cytoplasmic organelles such the endoplasmic reticulum, according to Ghadially [21]. The study's electron microscopic results in group II confirmed the vacuolation of Sertoli cells.

The prior research [22] suggested that vacuoles of Sertoli cell indicated direct impairment to this cell and highlighted its initial reaction to harm. It was clarified that the autophagosomes' formation caused the vacuolation, which allowed Sertoli cells to phagocytize dead germ cells [23]. Another further explanation for vacuolated Sertoli cells could be the expansion and aggregation of membranous organelles such as the ER [24].

Our results concerning Group III agreed with Daoud et al. [25] who reported that nanoparticles, such as ZnO, possess properties that can reduce oxidative stress and improve histological outcomes in testicular tissues. Their use has been associated with decreased collagen deposition in models of induced toxicity.

These findings also came in parallel with Perumal et al. [26] who described that rats given CP with subsequent administration of antioxidants showed improvements in histopathological parameters, down-regulated fibrosis and preserved spermatogenesis. They concluded that antioxidant therapies can counteract the fibrogenic effects of CP.

These nanoparticles have been studied for their protective effects in several biological systems, including their role in down-regulating oxidative stress and inflammation in different organ systems. Recent studies have suggested that ZnO-NPs may play a protective role against chemotherapeutic-induced toxicity, although their specific effects on testicular tissue remain underexplored [27].

However, other studies have reported adverse effects of ZnO-NPs, suggesting that their impact on testicular tissue is dose- and duration-dependent. Hosney et al. [28] observed that rats exposed to high doses led to severe damage, including deteriorated seminiferous tubules, abnormal germ cells with deeply stained pyknotic nuclei, desquamation, increased Sertoli cells, and interstitial vacuolation. These variations could be attributed to differences in ZnO-NP concentration, as high doses have been associated with oxidative stress rather than antioxidant protection [29].

Similarly, Almansor et al. [30] and Pinnho et al. [31] emphasized the potential cytotoxic effects of ZnO-NPs, informing that they can destruct and even disrupt cellular membranes, leading to destruction of Sertoli cells and germ cells.

In contrast to our findings, Mozaffari et al. [32] found that ZnO-NPs did not significantly affect tunica albuginea thickness, but they increased the number of degenerated seminiferous tubules. This can be attributed to variations in nanoparticle size, surface modifications, and administration routes, all of which influence their biological interactions and toxicity [33].

Moreover, while some studies observed a protective effect, others, such as Ahmed et al. [33], reported significant histopathological changes in ZnONP-exposed rats, including disorganization of seminiferous tubules, thickened and separated BM, widened interstitial tissues, congested vasculature, and pyknotic germ and Sertoli cells. The ultrastructural findings further confirmed these alterations, showing extensive degeneration of Sertoli cells, spermatogonic cells, and interstitial cells. This suggests that the duration of

exposure and the ability of testicular tissue to metabolize ZnO-NPs may also play a role in determining whether they exert protective or toxic effects.

Overall, the findings indicate that ZnONPs have a dual effect on testicular tissue, acting as a protective agent at lower doses and durations but potentially exerting toxic effects at higher doses and prolonged exposure. This highlights the need for careful dose optimization and further investigation into the mechanisms underlying their action.

In agreement with our results concerning Group IV, Vitamin E may have defensive properties against CP-induced testicular deterioration, according to a study by Omar et al. [34] that studied the protective effects of vitamin E in CP-induced toxicity. They found that these antioxidant molecules reduced cellular injuries associated with CP administration.

Hosney et al. [28] observed that rat testes sections treated with vitamin E displayed testicular histoarchitecture that was almost normal, which is consistent with our findings. Rats given vitamin E had seminiferous tubule structures and spermatogenic cell series that resembled those of control groups.

In accordance with our findings, Pearcce et al. [35] suggested that vitamin E might contribute to improve semen quality and, consequently, fertility. This could be achieved by reducing apoptosis and DNA disintegration and increasing sperm quality. These findings showed that oxidative stress and metabolic endotoxemia might be a major cause of sperm DNA damage in obese males.

In parallel with us, Ziamajidi et al. [36] demonstrated that antioxidants like vitamins A, C, and E could ameliorate testicular damage caused by oxidative insult from various agents, including nanoparticles. The study found that these vitamins significantly reduced collagen deposition in testicular histology after exposure to harmful substances like ZnO-NPs.

According to other researchs, vitamin E lowers endothelial cell toxicity and CP-induced nephrotoxicity and contains tocopherol, tocotrienol, and free radical scavengers [37, 38]. Vitamin E prevents free radical injury to the fatty acids that comprise unsaturated phospholipid membranes and may act as an inhibitor of lipid peroxidation reactions [38, 39, 40].

In accordance with us, Ali et al.[41] demonstrated that antioxidants like selenium can protect testicular tissue from toxic effects, resulting in decreased collagen deposition compared to control groups. This aligns with our findings regarding the defensive properties of vitamin E and ZnO-NPs against CP -induced damage.

In agreement with results of Group V, Xia et al. [42] stated that combination of zinc and vitamin E enhance the improvement of testicular tissue and spermatid against oxidative factors. The adding of vitamin E to ZnO-NPs has enhanced its capacity to combat oxidative damage, according to a study by Abd Elmonem et al. [43]

Collagen deposition in the testis can be predisposed by various factors, including oxidative stress, inflammation, and cellular signaling pathways. CP is known to induce oxidative stress, leading to cellular damage and subsequent fibrotic changes. However, ZnO nanoparticles overcome this oxidative stress and inflammation, thereby decreasing collagen synthesis [44, 45].

Additionally, vitamin E is an antioxidant that protects against oxidative damage and may help maintain normal collagen metabolism. The significant reduction in collagen fiber deposition observed in the combination treatment groups suggests a synergistic effect that helps preserve testicular architecture and function [46].

The limitations of the study were that the study utilized a limited number of adult albino rats, which may affect the statistical power and generalizability of the findings. The treatment duration of four weeks may not be sufficient to observe long-term effects or recovery patterns following CP -induced injury and although protective effects were observed, the potential toxicity of ZnO-NPs at higher concentrations was not thoroughly investigated.

Conclusion

Zinc oxide nanoparticles and Vitamin E, either alone or in combination, can effectively protect the testes against cisplatin-induced injury by ameliorating oxidative stress and preserving testicular structure and function. With little differences in their effectiveness: the effect of ZnO-NPs is better than Vitamin E, but their combined use revealed more increase in efficiency than ZnO-NPs alone. These findings suggest a potential therapeutic application of ZnO-NPs and Vitamin E in mitigating cisplatin-related testicular toxicity.

Therefore, future studies should involve larger number of animals and longer durations. Dose optimization is recommended to ensure efficacy and minimize ZnO-NPs toxicity.

Sources of funding

This study has not been funded.

Author contribution

Authors contributed equally to the study**.**

Conflicts of interest

No conflicts of interest

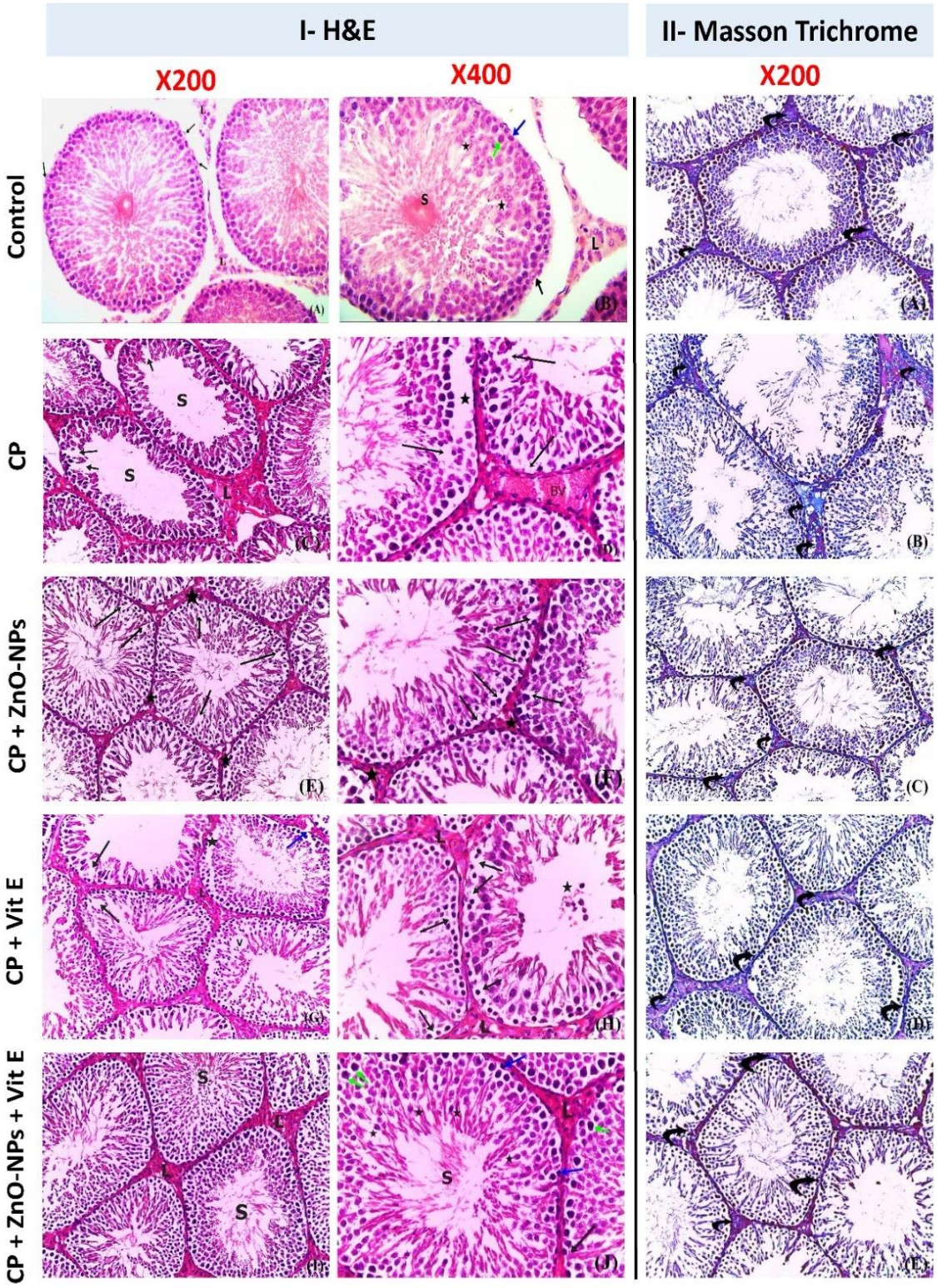

Figure 1: (I) H&E (X200 & 400), A photomicrograph of a section in testis of an adult male albino rat's testis. (A,B) Control group showing (A): normal seminiferous tubules with regular outline showing myoid cell (black ↑). The tubules densely packed with spermatogenic cells and normal interstitial tissue containing Leydig cell (L) in between, (B): magnified seminiferous tubules with interstitial tissue among

them. The seminiferous tubule lined with Sertoli cell (black ↑), Spermatogonia laying on BM (blue ↑), primary spermatocyte (green ↑), Round spermatid (star) and spermatozoa (S). The interstitial tissue contains clumps of Leydig cells (L) with oval or rounded nuclei and pale eosinophilic cytoplasm. **(C,D) Cisplatin group showing**, (C): destruction in the testicular tissue, with apparent decrease in spermatozoa population (S) and areas of cell loss (↑) between the spermatogenic cells. The interstitial tissue (L) showing exudate with dilated and congested blood vessels, (D): detached basement membrane in the seminiferous tubule epithelium (star) and multiple areas of cell loss (↑) between the spermatogenic cells. The interstitial tissue shows dilated and congested vasculature between the tubules (BV). **(E,F): (Cisplatin + ZnO-NPs) group showing,** (E): some changes with regular outline of the majority of seminiferous tubules. The tubules are packed together and lined with stratified germinal epithelium with some areas of cell loss (↑). The interstitial tissue between the tubules containing dilated vasculature and exudate fluid (star). (F): vacuolations (arrow) in spermatogenic cells in the germinal epithelium. The interstitial tissue between the tubules has congested blood vessels and exudate fluid (star). **(G,H): (Cisplatin + Vitamin E) group showing**, (G): disturbed architecture of the seminiferous tubules with corrugated outlines. Some tubules show areas of spermatogenic cell loss (black↑), discontinuation of basement membrane (blue↑) and areas of vacuolations (V) and separation (star). The interstitial tissue shows exudate fluid and congested blood vessels (L). (H): shedding of cells into the lumen (star) and areas of vacuolations (↑) between the spermatogenic cells in the germinal epithelium. The interstitial tissue between the tubules containing exudate fluid and inflammatory cells (L). **(I,J): (cisplatin + ZnONPs + Vitamin E) group showing,** (I): nearly regular assembly of seminiferous tubules with ordered outlines and packed with spermatogenic cell and the lumen displaying spermatozoa (S) with interstitial tissue (L) in between. (J): apparently normal seminiferous like control group. The seminiferous tubule displays Sertoli cell (black ↑), Spermatogonia (blue↑) laying on basal lamina, 1ry spermatocyte (green ↑), Round spermatid (star), spermatozoa (S). The interstitial tissue in between contains Leydig cells (L).

(II) Masson trichrome (X200)*:* (**A): Control group showing:** the regular spreading of fine collagen fibers (curved ↑) at the BM of seminiferous tubules, perivascular, and in between the tubules. **(B): cisplatin group showing:** increased deposition of dense collagen fibers (curved ↑) at the BM of seminiferous tubules, in the wall of vasculture and peri-tubular. **(C): (Cisplatin + ZnO-NPs) group showing**: collagen fibers accumulation (curved ↑) at the BM of seminiferous tubules and in-between the tubules. (**D): (Cisplatin + vitamin E group) showing**: increased accumulation of collagen fibers (curved ↑) at the BM of seminiferous tubules, around the dilated ,congested vasculature and in-between the tubules. **(E): (Cisplatin + ZnONPs + vitamin E group) showing:** negligible buildup of fine collagen fibers (curved ↑) at the BM of seminiferous tubules, peri-vascular and in-between the tubules.

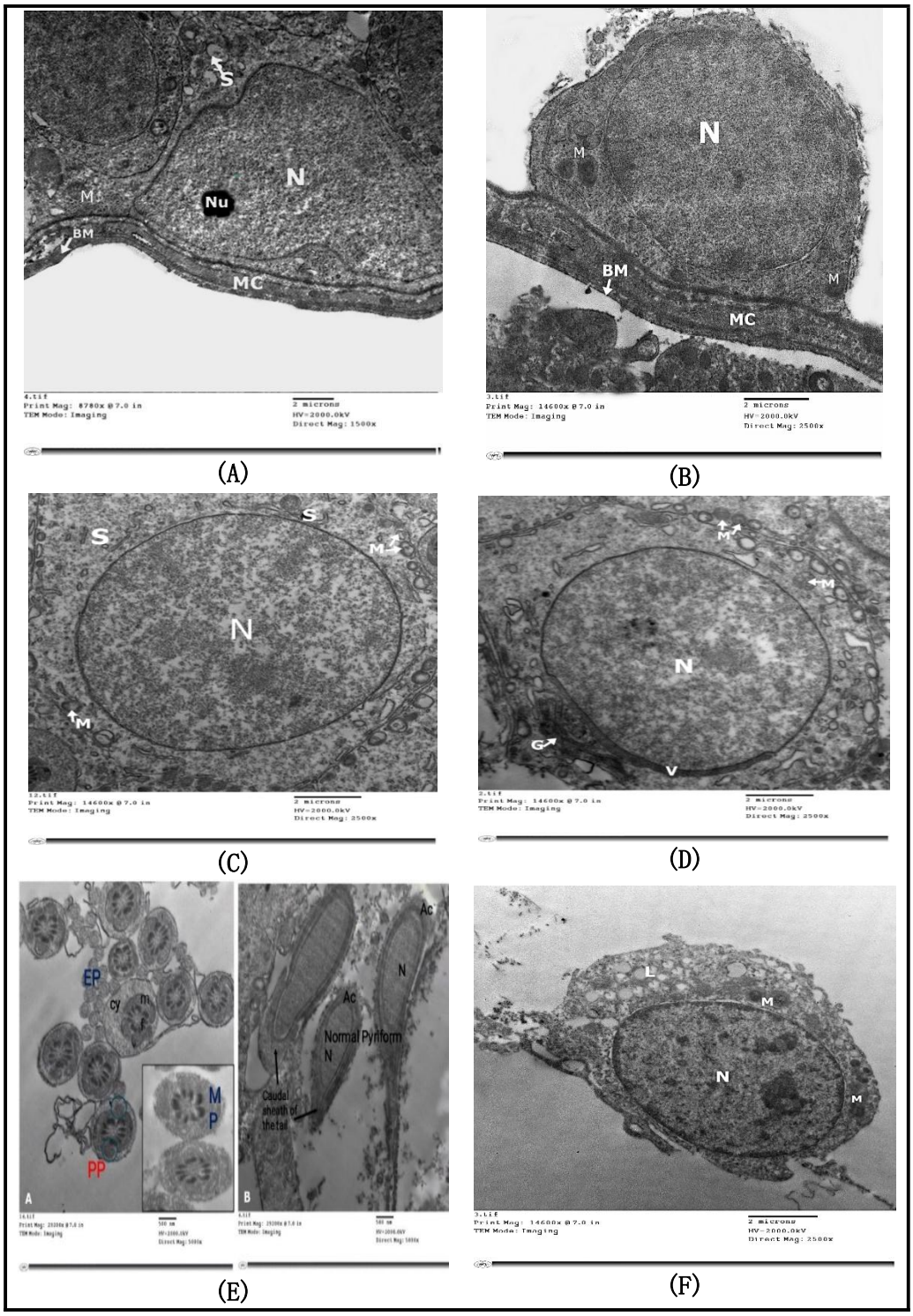

Figure 2: In group I (control) group (A): Sertoli cell laying on thin regular BM, surrounded by flat myoid cell (M.C). Sertoli cell showing typical indented nucleus (N) with noticeable eccentric nucleolus (Nu). Its cytoplasm has mitochondria (M) and SER (S) (TEM X 1500), **(B):** spermatogonia cell lying on BM surrounded by flat myoid cell (M.C). The cell showing ovoid nucleus (N) with regular nuclear envelop and multiple mitochondria (M) (TEM X 2500), **(C):** primary spermatocyte with big, circular nucleus (N) with electron dense chromatin, many mitochondria (M) and cisternae of smooth ER (S) (TEM X 2500), **(D):** spermatid with pale rounded nucleus (N), plentiful peripheral mitochondria (M) with electron lucent

center, acrosomal vesicle (V) elaborated by large Golgi apparatus (G) (TEM X 2500), **(E):** sperm depict the middle pieces (MP), the principal piece (PP), the end piece (EP), cytoplasm(cy) and mitochondrial sheath (m). B) Longitudinal sections in sperms depict the pyriform nucleus (N), acrosomal cap (AC) and caudal sheath of the tail (TEM X 5000), **(F)** Leydig cell with oval euchromatic nucleus (N) with clusters of heterochromatin. The cytoplasm has many fat droplets (L) of dissimilar sizes and numerous mitochondria (M) (TEM X 2500)

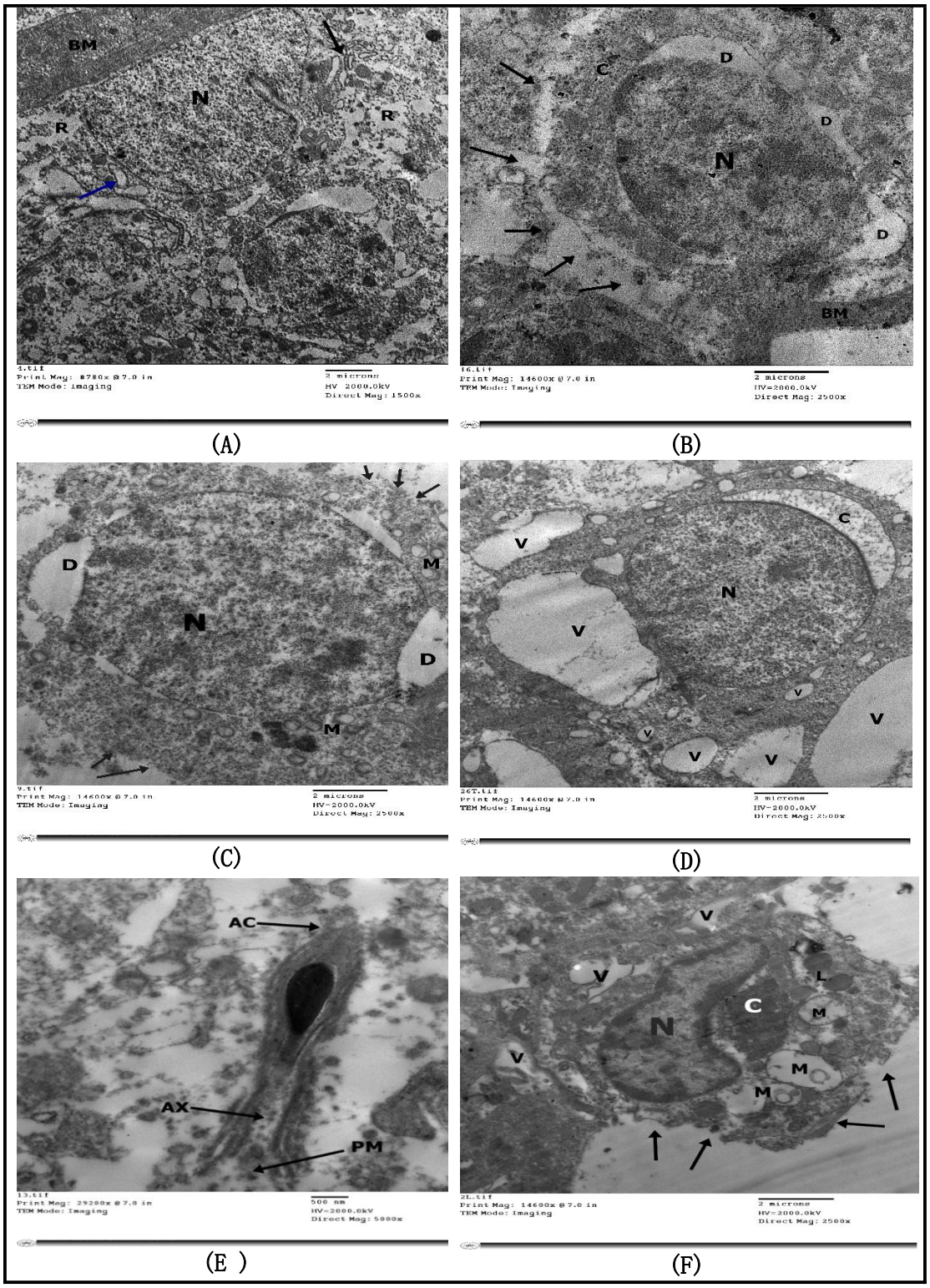

Figure 3 : In Group II (cisplatin group), (A): thickened BM and Sertoli cell with degenerating nuclei and disintegrated chromatin (N), areas of rarified cytoplasm (R), swollen cisternae of SER (black↑), ballooned mitochondria with lost cristae (blue ↑) (TEM X 1500), **(B):** Spermatogonium rested on thick irregular basement membrane (BM). The cytoplasm is dark with ill-defined organelles(C) and ill-defined cell boundary (arrow). The nucleus (N) is shrunken and irregular with perinuclear dilatation (D) (TEM X

2500), **(C):** 1ry spermatocyte with widespread patches of heterochromatin in their nucleus (N) and focal dilatations of the nuclear membrane (D). The cytoplasm shows numerous mitochondria (M) and ill-defined cell boundary (arrow) (TEM X 2500), **(D):** distorted early spermatid with irregular nuclei (N) and dilated acrosomal cap (C). The cytoplasm shows degeneration and multiple huge vacuolations (v) and ill-defined cell boundary (TEM X 2500), **(E):** longitudinal section of sperm with focal distortion of acrosomal cap (AC), disassembled axoneme with extrusion of its content (AX) and broken plasma membrane (PM)(TEM X 5000) **, (F):** Leydig cell with disrupted cell boundary (arrow) and indentation of the nucleus and condensed chromatin (N). The cytoplasm shows condensation (C), vacuolations (V) and decreased lipid content (L). Also, there is ballooned mitochondria with destructed cristae (M) (TEM X 2500)

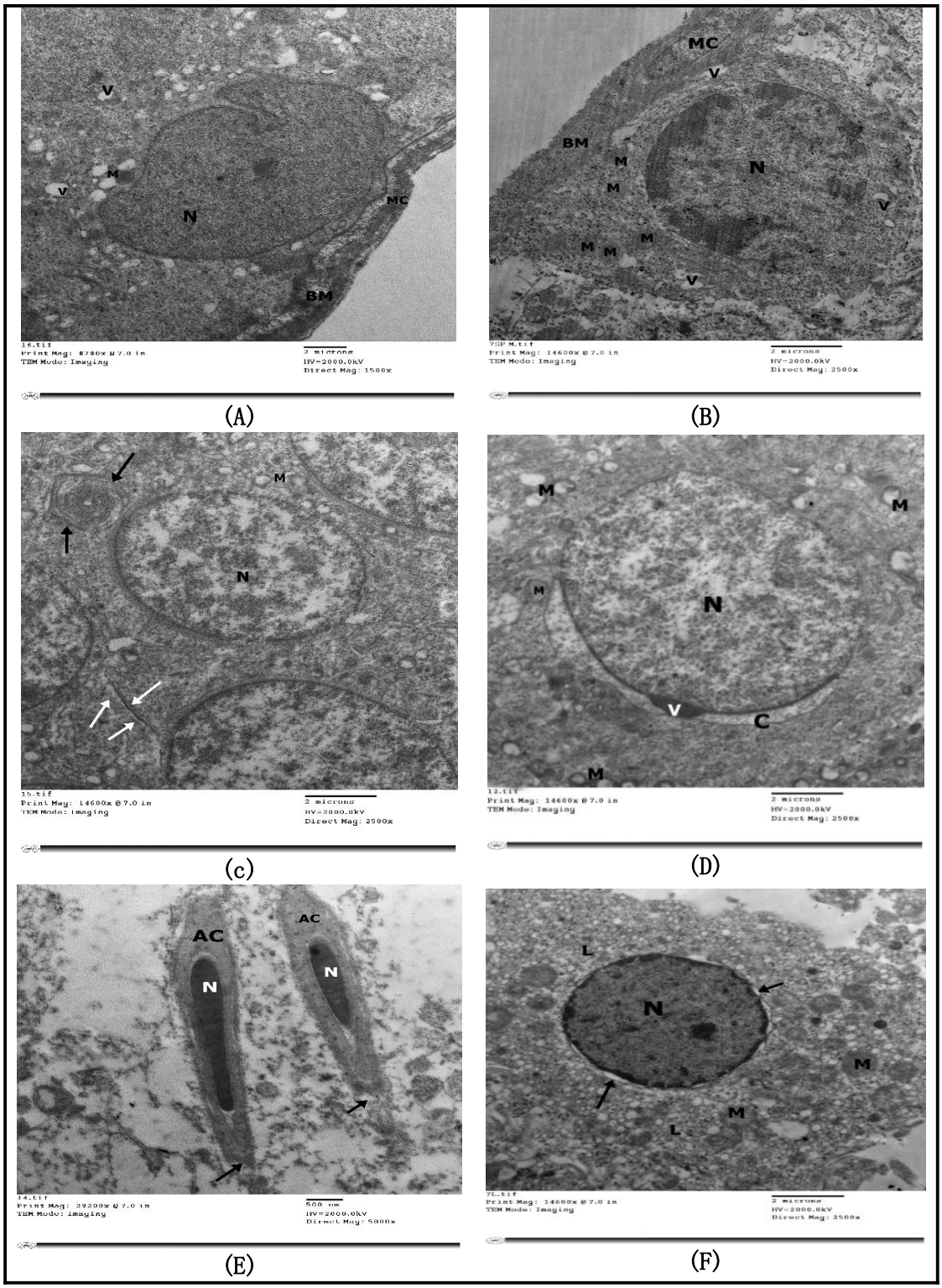

Figure 4: In Group III (cisplatin + ZnO-NPs group), (A): Sertoli cell resting on irregular thick BM and surrounded by flat myoid cell (M.C). It has normal indented nucleus (N) with noticeable nucleolus. Its cytoplasm displays mitochondria (M) but some vacuolations are still depicted (V) (TEM X 1500), **(B):** spermatogonia cell lying on basement membrane (B.M.) surrounded by flat myoid cell (M.C). The cell showing circular nucleus (N), with condensed chromatin along the nuclear envelope, multiple mitochondria

(M) and some vacuolations (V) (TEM X 2500), **(C):** some nuclei of primary spermatocytes with prominent tight junction between cells (white↑). The nucleus is large, rounded (N) with electron dense chromatin. There are also some swollen mitochondria (M) and an autophagosome as a sign of improvement (black ↑) (TEM X 2500), **(D):** early spermatid with nearly rounded nucleus (N), an abnormally dilated acrosomal cap (C) and acrosomal vesicle (V) and numerous peripherally arranged mitochondria (M) but swollen with destructed cristae (TEM X 2500), **(E):** longitudinal section of sperm showing normal acrosomal cap (AC) and pyriform nucleus (N) but tail distortion still depicted (arrows) (TEM X 5000**), (F):** Leydig cell with circular nucleus (N) with marginated heterochromatin and surrounded by small focal dilatations of nuclear membrane (arrows). The cytoplasm has several lipid droplets (L) of dissimilar sizes and numerous mitochondria (M) (TEM X 2500)

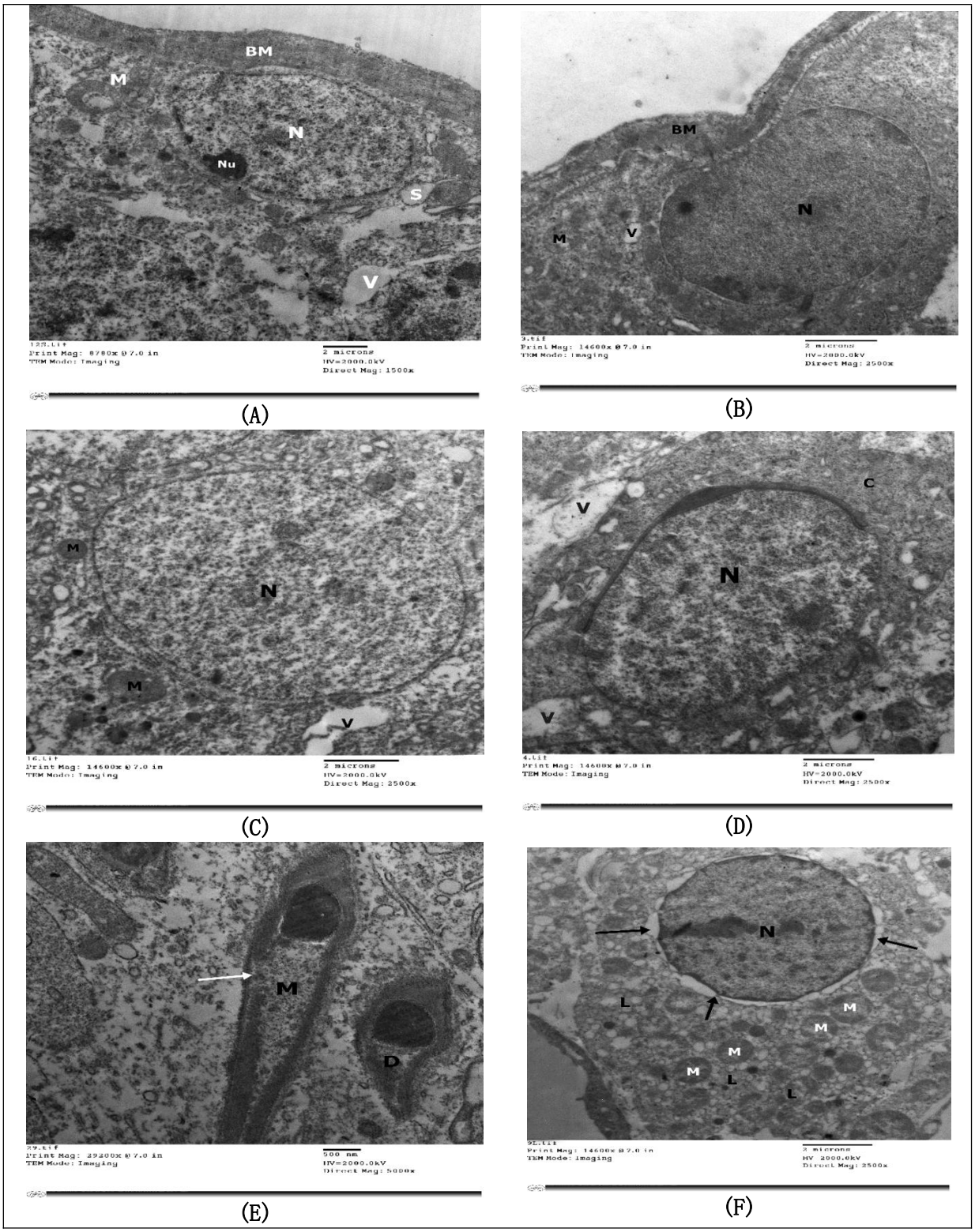

Figure 5: In Group IV (cisplatin + vitamin E group), (A): Sertoli cell resting on slightly thickened BM. The nucleus (N) doesn't have typical shape but with noticeable nucleolus (Nu). The cytoplasm still degenerated with areas of vacuolations (V). Some mitochondria (M) and sER (S) are still swollen (TEM X 1500), **(B):** spermatogonia cells lying on irregular BM. The cell showing ovoid nucleus (N), with focal

condensed chromatin along the nuclear envelope. The cytoplasm shows mitochondria (M) and vacuolation (V) (TEM X 2500), **(C):** 1ry spermatocyte with slightly oval nucleus (N). The cytoplasm shows vacuolations (V) and distended mitochondria (M) (TEM X 2500), **(D):** early spermatid with oval nucleus (N) and acrosomal cap and vesicle. The cytoplasm (C) is ill-defined with ill-defined organelles and multiple vacuoles (V) (TEM X 2500), **(E):** longitudinal sections of sperms with abnormal middle piece (M) of one sperm and an area of disassembly (white ↑). Another deformed spermatozoon (D) with small nucleus and abnormal acrosomal cap (TEM X 5000), **(F):** Leydig cell nucleus (N) is rounded with focally dilated nuclear envelop (↑). The cytoplasm has several lipid droplets (L) of dissimilar sizes and numerous swollen mitochondria (M) (TEM X 2500)

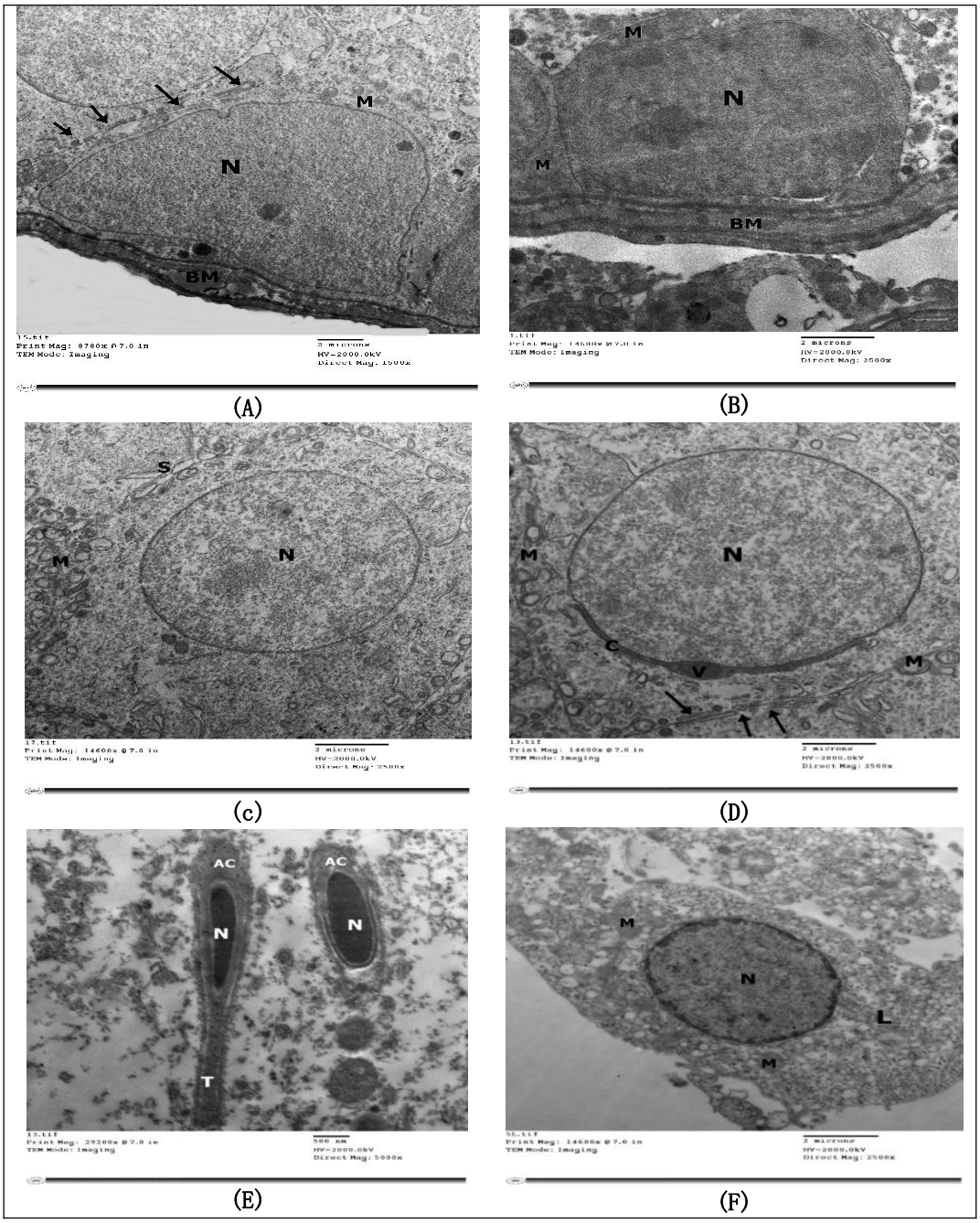

Figure 6: In Group V (cisplatin + ZnONPs + vitamin E group), (A): nearly normal Sertoli cell on thin BM. Sertoli cell showing indented nucleus (N) with noticeable nucleolus. The cytoplasm has mitochondria (M). Note prominent tight junction between cells (arrow) (TEM X 1500), **(B):** Spermatogonia cell lying on basement membrane (B.M.). The cell showing ovoid nucleus (N), slightly swollen mitochondria (M) (TEM X 2500), **(C):** primary spermatocyte with big, rounded nucleus (N) and slightly swollen mitochondria (M) and cisternae of sER (S) (TEM X 2500), **(D):** spermatid with pale rounded nucleus (N), abundant peripherally organized mitochondria (M) with electron lucent center, acrosomal vesicle (V) and acrosomal cap (c). Note intercellular junctions between cells (arrows) (TEM X 2500), **(E):** nearly normal longitudinal sections in sperms depict the pyriform nucleus (N), acrosomal cap (AC) and tail (T) (TEM X 5000), **(F):** apparently normal Leydig cell with ovoid euchromatic nucleus (N) with marginated heterochromatin. The cytoplasm has many fat droplets (L) of variable sizes and numerous mitochondria (M) (TEM X 2500)

References

1. Sharma RK, Bareja S. Zinc oxide nanoparticles: Chemical and green synthesis, characterization, and comparative evaluation of their effects on caprine testis in vitro. J Biochem Mol Toxicol. (2022);36:67-80.
2. Shamhari MN, Wee SB, Chin FS, Kok YK. Synthesis and characterization of zinc oxide nanoparticles with small particle size distribution. Acta Chim Slov. (2018);65:578-85.
3. Liao C, Jin Y, Li Y, Tjong SC. Interactions of zinc oxide nanostructures with mammalian cells: Cytotoxicity and photocatalytic toxicity. Int J Mol Sci. (2020);21:95-9.
4. Erfani Majd N, Hajirahimi A, Tabandeh MR, Molaei R. Protective effects of green and chemical zinc oxide nanoparticles on testis histology, sperm parameters, oxidative stress markers and androgen production in rats treated with cisplatin. Cell Tissue Res. (2021);384:561-75.
5. Vickram S, Rohini K, Srinivasan S, Veenakumari DN, Archana K, Anbarasu K, et al. Role of zinc (Zn) in human reproduction: A journey from initial spermatogenesis to childbirth. Int J Mol Sci. (2021);22:21-88.
6. Kaya K, Ciftci O, Cetin A, Doğan H, Başak N. Hesperidin protects testicular and spermatological damages induced by cisplatin in rats. Andrologia. (2015);47:793-9.
7. Rahimi A, Asadi F, Rezghi M, Kazemi S, Soorani F, Memariani Z. Natural products against cisplatin-induced male reproductive toxicity: A comprehensive review. J Biochem Mol Toxicol (2022);36:56-76.
8. Beytur A, Ciftci O, Oguz F, Oguzturk H, Yilmaz F. Montelukast attenuates side effects of cisplatin including testicular, spermatological, and hormonal damage in male rats. Cancer Chemother Pharmacol. (2012);69:13-27.
9. Ibrahim MA, Bakhaat GA, Tammam HG, Mohamed RM, El-Naggar SA. Cardioprotective effect of green tea extract and vitamin E on Cisplatin-induced cardiotoxicity in mice: Toxicological, histological and immunohistochemical studies. Biomed Pharmacother. (2019);113:731-50.
10. Feng Y, Huang X, Duan Y, Fan W, Duan J, Wang K, et al. The effect of vitamin e and metallothionein on the antioxidant capacities of cadmium-damaged liver in grass carp ctenopharyngodon idellus. Biomed Res Int. (2018);2018:79-88.
11. Altındağ F, Meydan İ. Evaluation of protective effects of gallic acid on cisplatin-induced testicular and epididymal damage. Andrologia. (2021);53:9-20.
12. Shakibaie M, Forootanfar H, Jafari E, Salimi A, Doostmohammadi M, Rahimi H-R. Microwave-assisted synthesized zinc nanoparticles attenuate cisplatin-induced testicular toxicity in mice. Environ Toxicol Chem. (2020);102:386-98.
13. Layton C, Bancroft JD, Suvarna SK. Fixation of tissues. Bancroft's theory and practice of histological techniques. (2019). p. 23-5.
14. Hayat MA. Principles and techniques of electron microscopy. Principles and techniques of electron microscopy (2000). p. 30-40.
15. Abdel-Latif R, Fathy M, Anwar HA, Naseem M, Dandekar T, Othman EM. Cisplatin-Induced Reproductive Toxicity and Oxidative Stress: Ameliorative Effect of Kinetin. Antioxidants (Basel). (2022);11:30-40.
16. Li CY, Lin WC, Moonmanee T, Chan JP, Wang CK. The Protective Role of Vitamin E against Oxidative Stress and Immunosuppression Induced by Non-Esterified Fatty Acids in Bovine Peripheral Blood Leukocytes. Animals (Basel). (2024);14:30-50.

17. Ismail HY, Shaker NA, Hussein S, Tohamy A, Fathi M, Rizk H, et al. Cisplatin-induced azoospermia and testicular damage ameliorated by adipose-derived mesenchymal stem cells. Biol Res. (2023);56:2-20.
18. Miller MA, Zachary JF. Mechanisms and morphology of cellular injury, adaptation, and death. Pathologic basis of veterinary disease (2017). p. 20-54.
19. Ardiani A, Purnomo BB, Penta SK, Wantri AK, Wardhani V. Erythropoietin effect on testicular germinal epithelium cells in undescended testis mice model. Arch Med. (20210;75:168-90.
20. Gong Y, Wu J, Huang Y, Shen S, Han X. Nonylphenol induces apoptosis in rat testicular Sertoli cells via endoplasmic reticulum stress. Toxicol Lett. (2009);186:84-95.
21. Ghadially FN. Ultrastructural pathology of the cell and matrix: a text and atlas of physiological and pathological alterations in the fine structure of cellular and extracellular components: Butterworth-Heinemann; (2013). 35-87 p.
22. El Shafai A, Zohdy N, El Mulla K, Hassan M, Morad N. Light and electron microscopic study of the toxic effect of prolonged lead exposure on the seminiferous tubules of albino rats and the possible protective effect of ascorbic acid. Food Chem Toxicol. (2011);49:34-43.
23. Nashwa S W, Eman A AF, Fayza E A, Ebtehal Z H. Histological study of the effect of exogenous glucocorticoids on the testis of prepubertal albino rat. Egypt J Histol. (2010);33:53-64.
24. Hild SA, Reel JR, Dykstra MJ, Mann PC, Marshall GR. Acute adverse effects of the indenopyridine CDB-4022 on the ultrastructure of sertoli cells, spermatocytes, and spermatids in rat testes: comparison to the known sertoli cell toxicant Di-n-pentylphthalate (DPP). J Androl. (2007);28:21-9.
25. Daoud NM, Aly MS, Ezzo OH, Ali NA. Zinc oxide nanoparticles improve testicular steroidogenesis machinery dysfunction in benzo [α] pyrene-challenged rats. Sci Rep. (2021);11:11-67.
26. Perumal P, Sathakkathulla NA, Kumaran K, Ravikumar R, Selvaraj JJ, Nagendran V, et al. Green synthesis of zinc oxide nanoparticles using aqueous extract of shilajit and their anticancer activity against HeLa cells. Sci Rep. (2024);14:22-47.
27. Shabir S, Sehgal A, Dutta J, Devgon I, Singh SK, Alsanie WF, et al. Therapeutic Potential of Green-Engineered ZnO Nanoparticles on Rotenone-Exposed D. melanogaster (Oregon R(+)): Unveiling Ameliorated Biochemical, Cellular, and Behavioral Parameters. Antioxidants (Basel). (2023);12:33-54.
28. Hosney A, Khamis H, Ali H, Kheirallah N. Protective effects of Vitamin E against Zinc Oxide nanoparticles-induced histotoxicity of liver and testicular tissue, genotoxicity and biomarker stress in male albino rats. Res Sq. (2024):20-43.
29. Talebi AR, Khorsandi L, Moridian M. The effect of zinc oxide nanoparticles on mouse spermatogenesis. J Assist Reprod Genet. (2013);30:1203-9.
30. Almansour AI, Arumugam N, Prasad S, Kumar RS, Alsalhi MS, Alkaltham MF, et al. Investigation of the optical properties of a novel class of quinoline derivatives and their random laser properties using ZnO nanoparticles. Molecules. (2021);27:145-60.
31. Pinho AC, Morais PV, Pereira MF, Piedade AP. Changes in the antibacterial performance of polymer-based nanocomposites induced by additive manufacturing processing. Polymers. (2025);17:171-95.

32. Mozaffari A, Mirzapour SM, Rad MS, Ranjbaran M. Cytotoxicity of PLGA-zinc oxide nanocomposite on human gingival fibroblasts. J adv periodontol implant. (2023);15:28-33.
33. Ahmad S, Mfarrej MFB, El-Esawi MA, Waseem M, Alatawi A, Nafees M, et al. Chromium-resistant staphylococcus aureus alleviates chromium toxicity by developing synergistic relationships with zinc oxide nanoparticles in wheat. Ecotoxicol Environ Saf. (2022);230:113-42.
34. Omar S, Ahmed M, Khalil O, Mady MM. The possible ameliorative effects of vitamin E against cisplatin-induced injury on adult rat liver and testes. Eur J Anat. (2023);27:279-88.
35. Pearce C, Rychetnik L, Wilson A. The obesity paradigm and the role of health services in obesity prevention: a grounded theory approach. BMC Health Services Research. (2021);21:1-10.
36. Ziamajidi N, Khajvand-Abedini M, Daei S, Abbasalipourkabir R, Nourian A. Ameliorative effects of vitamins a, c, and e on sperm parameters, testis histopathology, and oxidative stress status in zinc oxide nanoparticle-treated rats. Biomed Res Int. (2023);2023:43-50.
37. Aggarwal BB, Sundaram C, Prasad S, Kannappan R. Tocotrienols, the vitamin E of the 21st century: its potential against cancer and other chronic diseases. Biochem Pharmacol. (2010);80:16-31.
38. Paksoy M, Ayduran E, Sanlı A, Eken M, Aydın S, Oktay ZA. The protective effects of intratympanic dexamethasone and vitamin E on cisplatin-induced ototoxicity are demonstrated in rats. Med Oncol. (2011);28:15-21.
39. Villani V, Zucchella C, Cristalli G, Galiè E, Bianco F, Giannarelli D, et al. Vitamin E neuroprotection against cisplatin ototoxicity: Preliminary results from a randomized, placebo-controlled trial. Head Neck. (2016);38:18-21.
40. Kalkanis JG, Whitworth C, Rybak LP. Vitamin E reduces cisplatin ototoxicity. Laryngoscope. (2004);114:38-42.
41. Ali AM, Shalaby SA, Abosaif GMM, Banna EA. Possible Protective Role of Selenium on Testicular Toxicity Induced by Bisphenol A in Adult Male Albino Rats: Histological and Immunohistochemical Study. Benha J Appl Sci. (2021);6:211-22.
42. Xia LZ, Liu LL, Yue JZ, Lu ZY, Deng RY, He X, et al. Ameliorative effects of zinc and vitamin E against phthalates-induced reproductive toxicity in male rats. Environ Toxicol. (2024);39:3330-40.
43. Abd Elmonem HA, Mahmoud AH, Abbas MM. Ameliorative effect of zinc oxide nanoparticles and vitamin E on some biochemical and histological changes in irradiated albino rats. Egypt J Radiat Sci Appl. (2021);34:1-10.
44. Dutta S, Sengupta P, Slama P, Roychoudhury S. Oxidative stress, testicular inflammatory pathways, and male reproduction. Int J Mol Sci. (2021);22:10-43.
45. Wiesmann N, Mendler S, Buhr CR, Ritz U, Kämmerer PW, Brieger J. Zinc Oxide Nanoparticles Exhibit Favorable Properties to Promote Tissue Integration of Biomaterials. Biomedicines. (2021);9:30-50.
46. Wang Z, Xu R, Yang H, Li R, Ding J, Chang Y, et al. Vitamin E Regulates the Collagen Contents in the Body Wall of Sea Cucumber (Apostichopus japonicus) via Its Antioxidant Effects and the TGF-β/Smads Pathway. Antioxidants (Basel). (2024);13:30-50.